Astron. Astrophys. 319, 67–73 (1997)

ASTRONOMY
AND
ASTROPHYSICS

HI observations of dwarf galaxies in voids⋆

W.K. Huchtmeier[1], **U. Hopp**[2], **and B. Kuhn**[3]

[1] Max-Planck-Institut für Radioastronomie, Auf dem Hügel 69, D-53121 Bonn 1, Germany
[2] Universitätssternwarte München, Scheiner Str.1, D-81679 München, Germany
[3] Max-Planck-Institut für Astronomie, Königstuhl 17, D-69117 Heidelberg, Germany

Received 6 October 1996 / Accepted 23 July 1996

Abstract. We report HI-observations of a sample of 43 optically selected galaxies from the Heidelberg-void project. Only emission line galaxies have been selected. The HI-detection rate was 67%. The observed sample is a mix in late-type morphology objects with a spread in luminosity. They were compared to other samples with similar selection effects and mixtures. The detected galaxies have a high HI content and their M_{HI}/L_B values are systematically higher than expected from a local field comparison sample. Especially, for the 10 dwarfs in our sample ($8.2 \leq log\, L_B \leq 9.2$) which appear to be highly isolated, a mean M_{HI}/L_B = 1.8 was derived which is higher than for *all* comparison samples, including those with the same restricted luminosity range. We discuss a *trend* in our data between the relative HI-content and the surrounding galaxy density holding from very high densities (Virgo-cluster) to the very isolated objects at the rims of the voids.

We also present HI observations of 7 HII-galaxies of the University of Michigan (UM) sample.

Key words: surveys – galaxies: ISM; distances and redshifts – large-scale-structure – galaxies: interactions – radio lines: galaxies

1. Introduction

Available galaxy catalogs all show a strong clustering of galaxies (radial velocities taken as a measure for their distance). This clustering to superclusters connecting individual clusters by narrow extended "strings" of galaxies leave large areas free of bright galaxies, the so called voids (e.g. Bahcall 1988). The discussion of the missing mass (i.e. dark matter) leads to models where the clustering of the visible matter is still pointing at the mass concentration but where the distribution of the dark matter might be quite smoother. In this context one could expect to find a certain number of faint (dwarf) galaxies within the voids (i.e. Dekel and Silk 1986). The actual galaxy density within voids has a cosmological implication and is of interest with respect to the formation of galaxies.

Galaxy catalogs are complete to a certain distance for big and bright galaxies but not for faint (dwarf) galaxies. In order to demonstrate typical void structures the velocity dimension needs to have a depth of $\sim 5000 kms^{-1}$ (e.g. Geller et al. 1989). So far this limit has not yet been reached for faint (dwarf) galaxies (Binggeli et al. 1990, Thuan et al. 1987, Tully 1988). Hopp et al. (1995) searched faint, low surface brightness galaxies by morphological criteria. This sample showed up to be dominated by emission line galaxies. Of the $\sim$ 175 galaxies with redshifts in this sample, we selected the most convincing 43 objects with redshifts below $11000 km\, s^{-1}$ for HI observations including nearly all of the very isolated ones found along the rims of the voids. This sample contains not only dwarf galaxies and is a mixture of late-type spirals, irregulars and low-surface-brightness (LSB) galaxies; like the Heidelberg-void sample, the galaxies are in areas of different galaxy density from cluster-sample via sheet sample to void sample. Our sample covers the luminosity range $8.2 \leq logL_B \leq 10.2$. We will consider dwarf galaxies all those galaxies with $8.2 \leq logL_B \leq 9.2$ ($-17.5 \leq M_{BT} \leq -15$).

There are several samples of dwarf galaxies available for comparison with the void sample. A sample of dwarf galaxies for a high galaxian density is the Virgo dwarf sample (Hoffman et al. 1987, 1989), while a sample for a lower galaxian density is the sample of nearby galaxies (Kraan-Korteweg & Tammann 1979 (KKT hereafter) , with $v_0 \leq 500 km\, s^{-1}$; for the HI parameter e.g. Huchtmeier & Richter, 1988, HR1 hereafter). Observations of low surface brightness galaxies (LSB) and blue compact dwarf galaxies (BCD) were taken from Staveley-Smith et al.(1992) and van Zee et al.(1995). For the comparison with our dwarf sample we will use only galaxies in the same luminosity range ($8.2 \leq logL_B \leq 9.2$) from these comparison samples.

In order to prepare a comparison sample of emission-line galaxies (ELG) we added a few galaxies from the University of Michigan objective-prism survey (UM, e.g. Salzer 1989).

Send offprint requests to: W.K. Huchtmeier
(huchtmeier@mpifr-bonn.mpg.de)

⋆ Tables 1 and 2 are also available in electronic form at CDS via ftp 130.79.128.5 or via http://cdsweb.u-strasbg.fr/abstract.html

2. HI-observations

The HI-observations were performed in 1994/95 with the 100m radiotelescope at Effelsberg which has a half-power-beamwidth of 9.3 ' at a wavelength of 21 cm. A cooled two channel HEMT receiver was followed by a 1024 autocorrelator which was split into four banks of 256 channels each. A total bandwidth of 6.25 MHz yielded a channel separation of 24.4 kHz which corresponds to a resolution of 6.25 $km\,s^{-1}$ or to 10.2 $km\,s^{-1}$ after Hanning smoothing. Observations were performed in the total power mode integrating 5 minutes on an empty (comparison) field ahead of the source followed by a five minute integration on the source. Source and reference data were combined to produce the profile. Typical total integration for the present profiles is one to two hours each. Position checks and calibration measurements were done by observing well-known radio continuum sources. Regular system checks were performed every few hours by observing well-known line sources. The *Toolbox* software of the MPIfR was used for the data reduction. There were no serious baseline problems due to observing at nighttime and using a smaller bandwidth. Only modest corrections using polynomials of first to third order were applied in the baseline correction procedure.

HI profiles of the detected galaxies are given in Fig. 1. Many of these profiles are narrow and single peaked, a typical feature of dwarf galaxies.

3. The data

In Table 1 we present the optical data as follows : The galaxy's name in column 1 is followed by the optical position (1950.0) in column 2, the apparent total blue and red magnitudes in columns 3 and 4, respectively. The blue diameters at a surface brightness of $25 mag./arcsec^2$, a_{25} and b_{25}, follow in columns 5 and 6, the redshift and its error in columns 7 and 8 [1]. The morphological classification (column 9) deviates from the usual system : a leading **lsb** marks a low-surface-brightness object, **S** marks a disk galaxy which can not be classified in more detail. **ed** is an edge-on disk. A parameter describing the galaxian density (gd) is given in column 10; details are given in a footnote to Table 1 [2].

Galaxies classified as ellipticals have not been detected in HI. The profile shown for the edge-on disk O0467-005 is very weak and uncertain. The identification of the galaxies with the observed HI emission is by agreement in position and in radial velocity (optical and radio) within the error range. The HI signal observed at the position of the S0 galaxy CGCG0021+1358 could be confused by an edge-on spiral at 3.6'. Hence the M_{HI}/L_B value of 0.14 should be considered as an upper limit. Similar cases are O0467-106 and O467-023. The HI emission of O0823-055 most probably is not confused by the E galaxy 5.2' away. VN2#274 and VN2#KOW363 are separated by only half a beamwidth, but in each case we find HI emission at the optical velocities which are very different for both galaxies. A2151-0033 is in a cluster environmont with several spirals in the beam which might contribute to the observed profile; the M_{HI}/L_B value is an upper limit. More information on possible confusion is given in the footnotes of Table 1.

In Table 2 the HI data are presented. The galaxy name in column 1 is followed by the total line flux in $Jy\,km\,s^{-1}$ (column 2), the peak flux (S_{max}) and its error (column 3), the heliocentric radial velocity of the HI-line (mean of the two midline velocities at a level of 25% and 20% of the peak) and its error in column 4, and the observed line width at a level of 50%, 25%, and 20% in column 5. The total HI-mass in column 6 was calculated as

$M_{HI} = 2.3610^5 D^2 \int S_v dv$,

where D in Mpc is the distance calculated from the redshift and the integrated HI-flux $\int S_v dv$ is in $Jy\,km\,s^{-1}$. The M_{HI}/L_B ratio is given in column 6. This parameter often is used to indicated the relative HI-content of a galaxy. Total B magnitudes have been corrected for galactic absorption following Burstein & Heiles (1978), and for the internal extinction following Sandage & Tammann (1987). Distances have been calculated assuming a Hubble flow with a constant H_0 = 75 $km\,s^{-1} Mpc^{-1}$. For the two galaxies without B magnitudes in Table 1 a typical B-R color has been assumed to calculate a B magnitude and the M_{HI}/L_B value given here.

4. Discussion

HI- and optical velocities agree within the errors derived for the optical velocities. Global parameters of the dwarf galaxies have been derived following the formulae given by (HR1, Huchtmeier & Richter, 1989 (HR2 from hereon)) for easy comparison with the nearby sample of galaxies (HR1) . The Virgo cluster dwarf sample (Hoffman et al. 1987, 1989) has been prepared the same way for comparisons with the present sample of dwarf galaxies in voids.

The morphology of the HI profiles (Fig. 1), i.e. the ratio between the linewidth at half power width (50% level) and the linewidth at the 20% level is the same as for the nearby sample of galaxies (HR1) within the errors. The Holmberg relation (e.g. Holmberg 1976, i.e. the correlation between linear diameter and the absolute blue magnitude as discussed by HR2) is followed by the void galaxies within the observational errors. The relation between total mass and the absolute blue magnitude follows the relation given by the comparison samples.

Our sample has been defined optically and selection follows morphological criteria. The high detection rate (67%) demonstrates that the bias due to the sensitivity limit is not severe. The relatively high observed values of M_{HI}/L_B establish that this sample is relatively HI-rich intrinsically. However, the following discussion assumes that the observed HI is part of the galaxy and not due to any kind of confusion, which ultimately has to be checked by high-resolution observations. The chance of con-

[1] A detailed surface photometry analysis of 22 of the galaxies presented here can be found in Vennik et al., 1996

[2] The parameter 'gd' is based on calculations of the nearest neighbourhood distances D_{NN} to the next galaxies as given by Kuhn (1994), see also Hopp & Kuhn (1995). The mean value of the D_{NN}'s increases with redshift due to the decreasing sampling in the catalogues, 'gd' takes this effect into account.

Table 1. Optical data

Galaxy	Position(1950) h m s	° ′ ″	m_B	m_R	$2a_{25}$ ″	$2b_{25}$ ″	z	dz	Type	gd*
CGCG0021+1358	00 21 36.0	13 58 00	15.40				0.01685	0.00051	SO	2
VN8#002	00 28 55.0	09 47 40	17.85	17.14	25	6	0.01593	0.00086	pec Irr	2
O0823-001	00 29 55.0	14 46 12	16.00				0.01809	0.00086	Sc	2
O0823-055	00 35 13.0	11 32 18	18.63	17.43	14	8	0.03116	0.00075	lsb Irr	6
O1274-017	00 54 08.0	13 57 06	17.99	16.98	18	12	0.03483	0.00102	S	5
CGCG1021-0024	10 21 36.0	00 24 00	16.03		22	10	0.02361	0.00107	S	6
CGCG1022-0036	10 22 00.0	-00 36 00	15.90		22	12	0.03363	0.00130	Sdm	5
O0467-106	10 24 58.0	-03 18 06		15.57	31	31	0.03159	0.00089	lsb Sdm	3
O0467-109	10 26 41.0	-03 18 42		17.19	27	19	0.02968	0.00055	Sdm	3
O0467-074	10 32 50.0	-01 21 42	17.28	16.48	65	54	0.02391	0.00028	lsb Irr	6
O0467-023	10 33 36.0	00 37 54	18.78	17.92	14	5	0.03519	0.00108	lsb Irr	5
O0467-061	10 35 40.0	-02 26 06	18.20	17.30	15	12	0.02045	0.00055	lsb Irr	2
O0467-009	10 36 43.0	00 01 12	17.32	16.32	31	14	0.02089	0.00256	Sd	2
O0467-005	10 38 28.0	00 53 24	17.22	15.48	28	7	0.02235	0.00080	Ed	5
O0467-014	10 39 50.0	01 23 18	17.35	16.61	27	14	0.02725	0.00045	lsb Sp	2
VN2#381	10 40 57.0	-00 19 18	18.40	17.29	15	9	0.01799	0.00029	Irr	2
VN2#274	10 42 08.0	-00 00 18	19.14	18.08	16	4	0.02846	0.00050	Irr	2
VN2#KOW363	10 42 10.0	00 04 07	17.41	16.47	21	12	0.01525	0.00095	lsb S	3
O0991-007	10 42 43.0	-04 55 36	18.43	17.48	11	6	0.02677	0.00047	lsb Irr	5
VN2#KOW213	10 42 50.0	-00 04 52	17.85	16.65	22	12	0.02581	0.00015	lsb S	3
VN2#KOW117	10 43 23.0	-00 10 36	18.49	17.62	9	8	0.01691	0.00065	lsb S	3
O0991-026	10 46 13.0	-04 08 54	15.82	14.69	28	24	0.02123	0.00055	SB	2
HN1278	10 47 59.0	-00 29 36	18.70	18.08	13	6	0.02546	0.00047	lsb Irr	4
HN1280	10 48 30.0	-02 06 36	15.38	14.37	24	20	0.02179		Sdm	3
O1397-049	10 51 47.0	02 27 36	17.96	17.34	18	12	0.02581	0.00024	lsb Irr	4
HN1306	10 53 25.0	00 15 54	16.77	15.93	23	10	0.02566	0.00121	Scd	4
VN4#158	13 04 50.0	34 02 30	17.55	16.36	30	8	0.03454	0.00036	pec ed	1
VN4#134	13 05 21.0	34 02 36	18.93	17.68	14	8	0.03301	0.00116	pec S	1
VN4#109	13 05 44.0	34 22 46	17.87	16.79	22	10	0.03260	0.00098	Sp	1
VN4#148	13 05 02.0	34 15 40	18.55	16.98	14	9	0.03477	0.00037	E/SO	1
VN4#080	13 06 24.0	34 10 35	18.02	17.07	16	13	0.03292	0.00010	lsb S	1
N VN4#071	13 08 01.0	34 15 58	17.48	16.18	38	09	0.03388	0.00021	ed	1
CGCG1305+3421	13 05 34.0	34 21 13	15.12	13.64	38	30	0.03359	0.00037	E	1
CGCG1305+3416	13 05 43.0	34 16 27	15.33	13.76	43	32	0.03324	0.00067	E	1
UGC8227	13 06 15.0	34 14 31	15.07	13.41	75	19	0.03385	0.00070	ed	1
O0083-166	15 59 20.0	16 45 00	18.26	16.97	15	5	0.01636	0.00078	lsb Sdm	2
O0083-187	15 59 43.0	16 53 24	17.02	16.04	22	16	0.03223	0.00041	Scd	1
A2151-0033	16 03 54.0	18 00 36	17.57				0.03590	0.00066	lsb Irr	1
A2151-0035	16 04 08.0	18 03 42	16.02				0.03483	0.00059	SO	1
O0083-110	16 06 44.0	17 37 48	17.01	15.88	23	18	0.03598	0.00067	lsb Sdm	1
Zw431.048	23 20 00.0	12 59 00	15.82	14.40	14	6	0.01311	0.00020	Sc	2
CGCG2357+0051	23 57 40.0	00 50 31	14.95		49	34	0.02527		pec Irr	3
CGCG2359+1104	23 58 57.0	11 04 04	15.10				0.03040	0.00083	Sc	5
UM92	01 15 59.0	02 11 29	18.51		10		0.02310			
UM348	01 35 48.0	01 38 48	18.18		6		0.02500			
UM372	01 47 35.0	02 03 38	15.16		50		0.00560			
UM454	11 45 43.0	-01 21 43	16.55		20		0.01261			
UM455	11 47 49.0	-00 15 01	17.10		14		0.01281			
UM467	11 52 55.0	-00 58 59	15.66		30		0.01938			
UGC7877	12 34 00.0	11 32 00	16.5		66	12	0.01971			

(*) 1 cluster; 2 sheet; 3 rim of sheet; 4 transition sheet-void; 5 rim of void; 6 void

CGCG0021+1358 - edge-on spiral of similar size at 3.9'
O0823-055 - E-type galaxy at 5.2'
CGCG1022-0036 - in group of four galaxies of similar size at 1.5', 4.6', and 6.9'; interaction with closest neighbour?
O0467-106 - spiral of similar size at 3.5'
O0467-023 - spiral of similar size at 3'
O0467-009 - elliptical galaxy at 1.8', foreground?
VN2#274 - VN2#K363 at 4.4', and a small (10") background spiral VN2#253 at 3.6'
VN2#KOW363 - VN2#274 at 4.4'
VN4#109 - CGCG1305+3421 (elliptical) at 2.6'
VN4#080 - UGC8227 at 5.7'
VN4#071 - nearby spiral VN#70 with different z (0.065) at 1.3'
CGCG1305+3421 - VN4#109 at 2.6'
CGCG1305+3416 - dE companion
UGC8227 - VN4#080 at 5.7' , VN4#069 at 4.4'
A2151-0033 - three spirals at 4.2', 4.9', and 6.4'
A2151-0035 - A2151-0035 at 4.5', other spirals at 3.7', and 2.6'

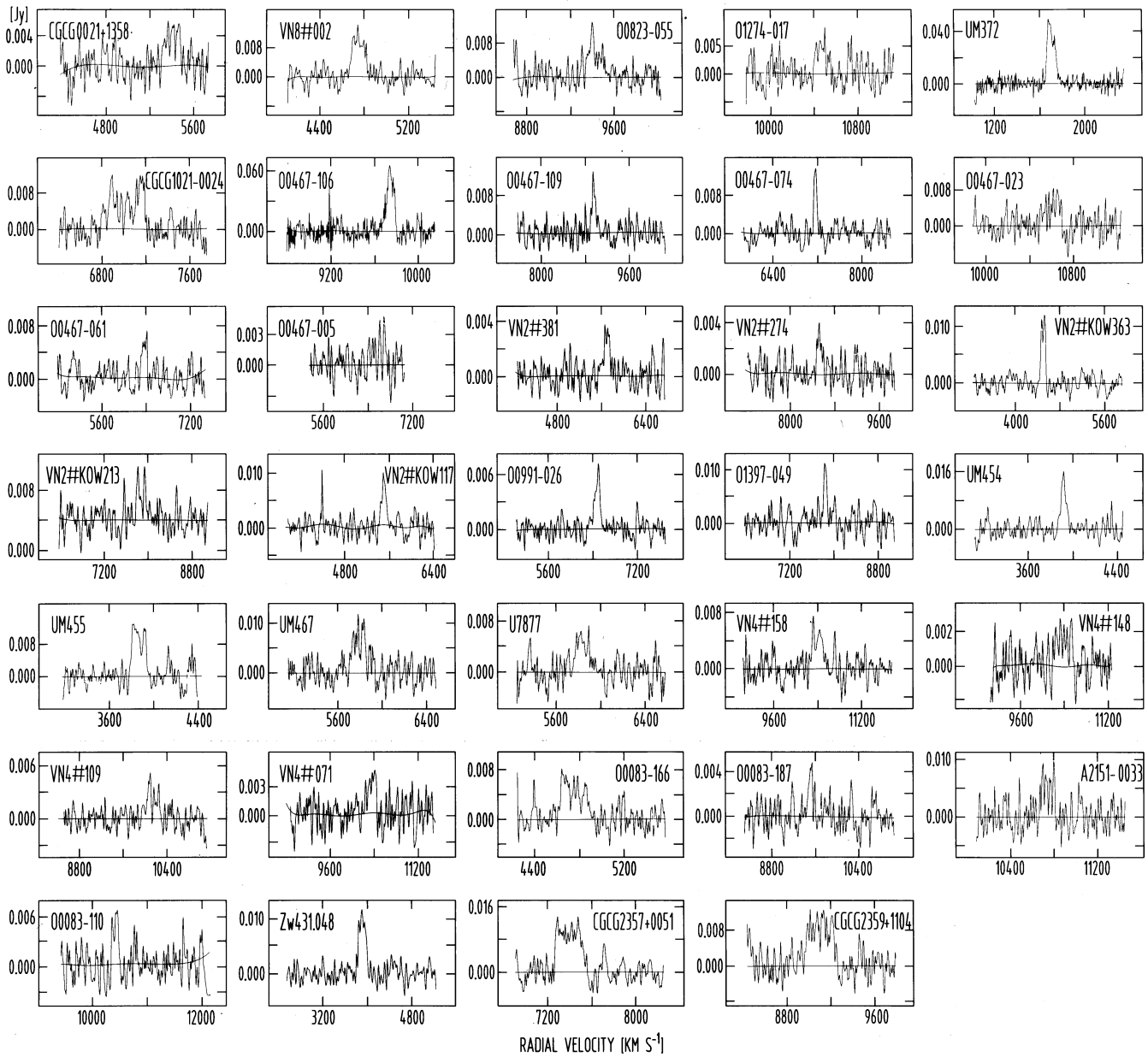

Fig. 1. HI spectra of dwarf galaxies in voids observed with the Effelsberg 100-m radiotelescope (9.3′ half power beam width). The spectrometer always was centered to the optical velocity; hence the difference optical minus radio velocity is directly given by the offset of the HI profile from the center of the spectrum. In general HI profiles of the present sample are weak; the signal for O0467-005 is uncertain.

fusion by nearby companions seems to be lower than expected earlier following the latest statement by Taylor et al. (1996). High resolution observations by de Blok et al. (1996) show no hints of confusion problems by nearby companions.

We do not want to repeat the lengthy discussion on what a dwarf galaxy is. Instead we will divide our sample into two luminosity ranges where objects in the range of fainter luminosities ($8.2 \leq logL_B \leq 9.2$) will be considered as dwarf. The comparison samples will be selected to be within the same luminosity range. In addition we will show the effect of different morphological types within this luminosity range.

The relation between HI mass and absolute blue magnitude as well as the relation between HI mass and linear diameter of the dwarf galaxies in voids agrees only for the bright/large galaxies with the comparison sample of nearby galaxies (HR1). The dwarfs ($8.2 \leq logL_B \leq 9.2$) in the present sample are richer in HI than expected from their luminosities or their linear sizes. In Fig. 2 we present the HI-mass to blue luminosity ratio M_{HI}/L_B versus blue luminosity L_B for the present sample. For this figure we reduced the blue magnitues in the same way as for the comparison samples (i.e. the correction for galactic absorption following Sandage & Tammann 1987). The difference in final M_{HI}/L_B and L_B for the two modes of correction

Table 2. HI-observations of dwarf galaxies in voids

Galaxy	HI flux $[Jy\ km\ s^{-1}]$	S_{max} [mJy]	HI velocity $[km\ s^{-1}]$	linewidth 50% 25% 20%	M_{HI} $[10^9 M_\odot]$	M_{HI}/L_B
27 CGCG0021+1358	0.66	6 ±1.9	5390 ±18	125 176 178	0.76	0.13
26 VN8#002	1.39	14 ±2.3	4748 ±15	116 153 160	1.42	1.79
28 O0823-001		±2				
29 O0823-055	1.2	12.9 ±2.3	9372 ±20	37 84 85	4.54	3.86
30 O1274-017	0.6	8.4 ±2.4	10449 ±25	61 109 112	2.68	0.99
31 CGCG1021-0024	2.16	11.9 ±2.3	7019 ±17	326 339 342	4.29	0.58
32 CGCG1022-0036		±4.6				
33 O0467-106	4.44	65.2 ±8.5	9746 ±5	75 90 93	16.00	2.03
01 O0467-109	1.13	13 ±2.0	8947 ±30	63 108 113	3.58	2.15
02 O0467-074	0.9	14 ±2.0	7160±17	62 80 84	1.83	0.85
34 O0467-023	0.8	8.6 ±2.2	10623 ±6	56 130 131	3.51	2.57
03 O0467-061	0.45	5±1.7	6354±24	121 130 132	0.66	0.99
35 O0467-009		±2.2				
04 O0467-005	0.4	4.3±1.2	6582±37	218 249 255	0.71	0.30
05 O0467-014		±1.6				
06 VN2#381	0.39	3.8±0.9	5703±30	104 114 118	0.44	1.00
07 VN2#274	0.37	4±1.0	8520±30	100 112 120	1.08	1.60
08 VN2#KOW363	0.94	12±1.3	4496±15	92 105 109	0.76	0.95
09 O0991-007		±1.8				
10 VN2#KOW213	0.92	7.1 ±1.7	7873 ±25	176 192 199	2.20	1.39
11 VN2#KOW117	0.72	9.6 ±1.8	5499±30	70 133 138	0.72	2.14
12 O0991-026	0.55	6.6 ±1.0	6479±25	85 133 140	0.88	0.12
13 HN1278		±1.9				
14 HN1280		±1.5				
15 O1397-049	0.95	10 ±1.5	7842 ±23	65 83 88	2.28	1.67
16 HN1306		±1.9				
17 VN4#158	1.08	7.5±1.6	10394 ±36	186 219 225	4.88	1.19
19 VN4#134		±2.9				
20 VN4#109	0.73	5.2 ±1.0	10142 ±35	214 248 252	2.94	1.18
18 VN4#148	0.49	3.4±1.1	10429 ±44	237 250 252	2.25	1.57
21 VN4#080		±3.4				
22 N VN4#071	0.69	4.7±1.7	10360±26	163 173 174	3.00	0.70
36 CGCG1305+3421		±2.4				
37 CGCG1305+3416		±1.8				
38 UGC8227		±1.6				
39 O0083-166	1.31	8.3±1.8	4714±20	167 182 188	1.38	2.59
23 O0083-187	0.48	4.7±1.2	9489±30	80 102 105	1.92	0.34
40 A2151-0033	0.72	9.7±2.3	10740±12	122 128 130	3.57	1.04
41 A2151-0035		±4.0				
24 O0083-110	0.33	6.6±1.7	10418±25	147 150 170	1.64	0.24
25 Zw431.048	1.53	11.7±1.4	3927±24	152 171 176	1.08	0.25
42 CGCG2357+0051	2.17	13.4±3.0	7390±15	230 267 271	5.43	0.24
43 CGCG2359+1104	2.43	12.8±2.8	9099±9	147 207 276	8.80	0.36
a01 UM 92		±2.0				
a02 UM 348		±1.6				
a03 UM 372	3.64	49.5±4.3	1700±6	82 100 106	0.47	0.58
a04 UM 454	0.76	16.1±2.0	3915±20	40 74 93	0.42	0.45
a05 UM 455	1.40	13.1±2.5	3863±20	134 150 155	0.80	1.39
a06 UM 467	1.12	11.8±2.2	5810±18	76 137 140	1.50	0.29
a07 UGC 7877	0.70	7.2±2.0	5820±20	131 150 158	1.0	0.27

(for galactic absorption) is always smaller than the size of the symbols in Fig. 2. Galaxies have been classified due to the density of their environment (gd in Table 1), void sample galaxies in a low galaxy density area are given by crosses (+), void sample galaxies in the "sheet" population are shown by open circles (o), and those belonging to a "cluster" population (i.e. galaxies in groups) are given by open triangles (△). The full line represents the smoothed mean values of the nearby galaxy sample (KKT). For the luminosity range covered by the void-sample dwarfs ($8.2 \leq logL_B \leq 9.2$) we give mean values in M_{HI}/L_B in Table 3 for the following (sub) samples where upper limits in M_{HI}/L_B have been considered, too (see Chamaraux, 1987):

i) the void sample of low galaxy density (gd=3 - 6),

ii) the void sample of higher galaxy density (sheet and small clusters) (gd=1-2),

iii-iv) the nearby galaxy sample (KKT) all types and type 10 only,

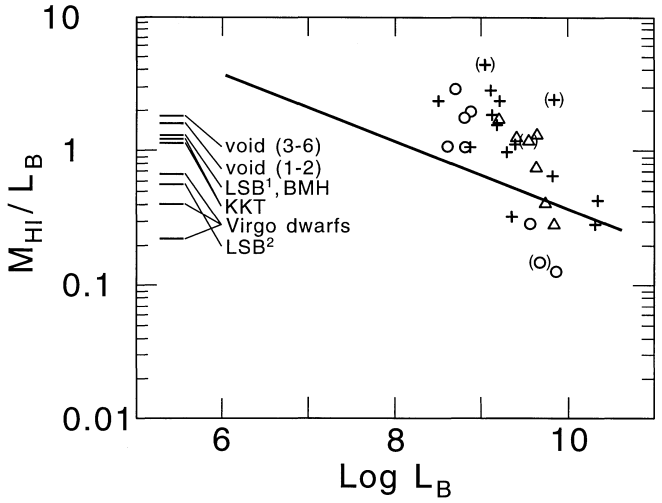

Fig. 2. The M_{HI}/L_B ratio in units of $M_\odot/L_\odot$ is given as a function of the blue luminosity (unit: $L_\odot$). Void sample galaxies of the cluster population (open triangles), galaxies from the sheet population (open circles), and galaxies from the void and rim of void population (crosses) are given by different symbols (see Table 3 for numerical values and sample sizes). The full line represents the smoothed mean values from the combined sample of nearby galaxies (Huchtmeier & Richter, 1988). Mean values of M_{HI}/L_B for the luminosity range given by the void sample are marked by the horizontal bars in the left hand side of the figure for our present sample and a number of comparison samples . Galaxies with possible confusion (Table 1) are given in parantheses.

Table 3. Average M_{HI}/L_B values for void subsamples and comparison samples for the luminosity range $8.2 \leq logL_B \leq 9.2$; for definition of 'gd' see text.

Sample	galaxy density 'gd'	sample size	M_{HI}/L_B
void	3-6	9	1.84 ± 0.25
void	1-2	9	1.50 ± 0.30
BMH [3]	2	11	1.27 ± 0.20
KKT	1-2	63	1.12 ± 0.14
KKT [4]	1-2	42	1.22 ± 0.19
LSB [1]	1-2	12	1.27 ± 0.72
LSB and BCD [2]			0.56 ± 0.6
Virgo dwarf	1	147	0.64 ± 0.35
Virgo dwarf [4]	1	62	0.40 ± 0.07
Virgo dwarf [5]	1	42	0.22 ± 0.03

1) van Zee et al. 1995
2) Staveley-Smith et al. 1992
3) de Blok et al. 1996
4) type 10 (Im, IBm) only
5) type 11 (BCD) only

v-vi) LSB samples (van Zee et al. 1995, Staveley-Smith et al. 1992) not considering those galaxies with extended HI distributions [3],

vii-ix) the Virgo dwarf sample (from Hoffman et al.1987,1989) in three different selections: all types, type 10, and type 11 (bcd's only).

This sequence of increasing galaxy density is a sequence of decreasing M_{HI}/L_B (see Table 3). However, as we noted above, our sample is biased by its selection criteria towards the presence of ISM (interstellar medium). We only selected emission line galaxies. In addition our sample is a mixture of different morphological types. For comparison M_{HI}/L_B values for the Virgo dwarf sample are given for all dwarfs in the selected luminosity range ($8.2 \leq logL_B \leq 9.2$), for type 10 (Im and IBm), and for type 11 (BCD galaxies) in Table 3. For the nearby sample (KKT) we consider all types and type 10 only for the given luminosity range ($8.2 \leq log\, L_B \leq 9.2$). The difference in M_{HI}/L_B for irregular galaxies only and for a type mix in the same luminosity range is not significant. Hence we might take these values for comparison with the void dwarfs, which is a sample of mixed types,too. The situation in the Virgo cluster is more complicated due to the cluster environment. Blue compact dwarf (BCD) galaxies seem to be compact in their HI dimensions, too, and seem to have moderate M_{HI}/L_B values (Staveley-Smith et al. 1992, van Zee et al. 1995, Table 3 for the Virgo cluster BCD's). Low surface brightness galaxies do not differ significantly in M_{HI}/L_B (e.g. van Zee et al. 1995, Staveley-Smith et al. 1992) except for the class of galaxies with extended HI halos (van Zee et al. 1995). None of our void galaxies shows excessive M_{HI}/L_B values as given by them (5.2 on the average) for LSB galaxies with extended HI haloes which are comparable to the situation in M83 (e.g. Huchtmeier and Bohnenstengel 1981) or NGC 262 (Heckman et al. 1982) and other extreme cases which are rather the exception (e.g. Briggs 1990). However, the presently available information on LSB galaxies refers to a rather small number of objects only. Because of the small number of objects involved in our void sample and the bias in selecting emission line galaxies (i.e. ISM available) a cautious remark is adequate. It is evident that the dwarfs in the present void sample are HI richer compared to the comparison samples. Galaxies in high density regions tend to have low values of M_{HI}/L_B while a decreasing galaxian density increases the probability for high M_{HI}/L_B parameters. If this trend proofs to be real it might reflect the greater chance of encounters for galaxies in a denser environment. It is interesting to note that the Virgo dwarf sample follows the sample of nearby galaxies with two exceptions: a) a small number of HI-rich galaxies are present, and b) a great number of HI-deficient dwarf galaxies (due to the cluster environment) are present.

Galaxies from the ELG comparison sample (UM galaxies) are located close to the reference line from the nearby galaxy sample (KKT). One of the undetected galaxies from the UM sample (UM348) is a BL-Lac candidate and shows no emission lines.

[3] van Zee et al. (1995) searched for LSB galaxies with extended HI halos; many of the galaxies in their list are HI-rich due to the presence of extended HI halos; hence they are not representative for the general galaxy population.

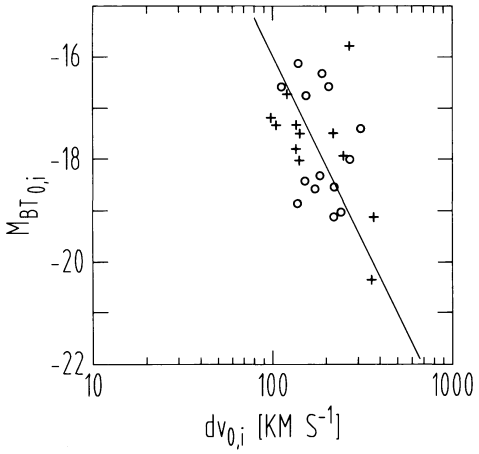

Fig. 3. The absolute blue magnitude M_{BT} of the void sample galaxies is plotted versus the corrected 21 cm line width dv_{0i}. Galaxies in areas of low galaxy density (gd code 3 to 6 in Table 1) are given by crosses (+), galaxies from higher density areas (gd code 1 and 2 in Table 1) are shown by open circles (o). The *Tully-Fisher relation* as derived by HR1 is given as a full line. The faintest galaxy in this plot is far away from the full line. This is the smallest object in our sample with a large inclination correction of its 21 cm line width.

In Fig. 3 we present the *Tully-Fisher* relation for the galaxies in areas of low galaxy density (gd parameter 3 to 6 in Table 1). The full line represents the TF as derived for the nearby sample of galaxies (HR1). The one aberrant point is the faintest object in this plot and the smallest object in our sample. It has a large inclination correction for its line width. In this case relative errors are quite large. All other galaxies are quite compatible with the full line, suggesting that our present distance scale does not need a great correction. However, the relative errors in blue magnitudes, HI line widths (e.g.see Fig. 1), and in the derived inclination values yield a considerable scatter which turns the TF relation for the present sample not into a very powerful tool for distance determinations.

5. Conclusions

HI observations of a subsample of 43 galaxies from the Heidelberg void sample yield M_{HI}/L_B ratios that are larger than expected from the nearby sample of galaxies for the luminosity of the galaxies. Most galaxies have single peaked narrow HI profiles typical for dwarf systems. There seems to be a tendency for the M_{HI}/L_B parameter to increase as the galaxy density decreases from the Virgo cluster dwarf sample to the void-sample by a factor of three on the average. The decrease of the M_{HI}/L_B ratio with increasing galaxy density seems reasonable as the chance of interaction between galaxies increases, too.

Acknowledgements. U.H. acknowledge the support by the Sonderforschungsbereich 375 of the Deutsche Forschungsgemeinschaft.

References

Bahcall, N.A., 1988, ARA&A **26**, 631
Binggelli, B., Tarenghi, M., Sandage, A., 1990, A&A **228**, 42
Briggs, F.H., 1990, AJ **100**, 995
Burstein, D., Heiles, C., 1978, ApJ **225**, 40
Chamaraux, P., 1987, A&A **177**, 326
de Blok, W.J.G., McGaugh, S.S., van der Hulst, J.M., 1996, MNRAS, in press
Dekel, A., Silk, J., 1986, ApJ **303**, 39
Geller, M.J., Huchra, J.P., 1989, Science **246**, 897
Heckman, T.M., Sancisi, R., Sullivan III, W.T., Balick, B., 1982, MNRAS **199**, 425
Hoffman, G.L., Helou, G., Salpeter, E.E., Glosson, J., Sandage, A., 1987, ApJS **63**, 247
Hoffman, G.L., Helou, G., Salpeter, E.E., Lewis, B.M., 1989, ApJ **339**, 812
Holmberg, E., 1976, in *Stars and Stellar Systems,* Vol. IX, eds. A.Sandage, M. Sandage, J. Kristian, Univ. of Chicago Press, p.123
Hopp, U., Kuhn, B., 1995, Review in Modern Astronomy **8**, 277
Hopp, U., Kuhn, B., Thiele, U., Birkle, K., Elsässer, H., Kovachev, B., 1995, A&AS **109**,537
Huchtmeier, W.K., Bohnenstengel, H.-D., 1981, A&A **100**, 72
Huchtmeier, W.K., Richter, O.-G., 1988, A&A **203**, 237 (HR1)
Huchtmeier, W.K., Richter, O.-G., 1989, A&A **210**, 1 (HR2)
Kraan-Korteweg, R.C., Tammann, G.A., 1979, Astron. Nachr. **300**, 181 (KKT)
Kuhn, B., 1994, Thesis University of Heidelberg
Salzer, J.J.: 1989 ApJ **347**, 152
Sandage, A., Tammann, G.A., 1987, *A Revised Shapley-Ames Catalog of Bright Galaxies* , Carnegie Institution, Washington
Staveley-Smith, L., Davies, R.D., Kinman, T.D., 1992, MNRAS **258**, 334
Taylor, C.L., Brinks, E., Grashuis, R.M., Skillman, E.D., 1996, ApJS **102**, 189
Thuan, T.X., Gott, J.R., Schneider, E., 1987, ApJ **315**, L93
Tully, R.B., 1988, AJ **96**, 73
van Zee, L., Haynes, M.P., Giovanelli, R., 1995, AJ **109**, 990
Vennik, J., Hopp, U., Kovachev, B., Kuhn, B., Elsässer, H., 1996, A&AS **117**, 261

This article was processed by the author using Springer-Verlag LaTeX A&A style file *L-AA* version 3.